

Syntheses, Structures and Reactivity of Electron-Rich Fe and Ru Complexes with the New Pentadentate Ligand Et₂NpyS₄-H₂ {4-(Diethylamino)-2,6-bis[(2-mercaptophenyl)thiomethyl]pyridine}

Dieter Sellmann,^{[a]†} Shaban Y. Shaban,^{*[a]} and Frank W. Heinemann^[a]

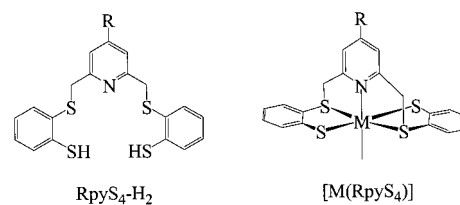
Keywords: Electron density / Iron / Nitrogenase / Ruthenium / S ligand

The new pentadentate thioether thiolate ligand Et₂NpyS₄²⁻ (= 4-(diethylamino)-2,6-bis[(2-mercaptophenyl)thiomethyl]pyridine(2-)) has been synthesised from dimethyl 4-bromopyridine-2,6-dicarboxylate by treatment with Et₂NH followed by reduction and tosylation. The tosylated product was subsequently used for the template alkylation of [Ni(S₂C₆H₄)₂]²⁻ to give [[Ni(Et₂NpyS₄)]₂] (4). Acidic hydrolysis of 4 resulted in the formation of the ligand Et₂NpyS₄-H₂·HCl (5). The dianion Et₂NpyS₄²⁻ reacted with FeCl₂·H₂O to afford the dinuclear high-spin species [[Fe(Et₂NpyS₄)]₂] (6) [μ_{eff} (297 K) = 5.15 μ_{B}]. Aerial oxidation of dinuclear 6 afforded the sulfinato complex [[Fe(Et₂NpyS₄-O₂)]₂] (7). Complex 6 proved to be a good precursor for the syntheses of [Fe(L)(Et₂NpyS₄)] [L = CO (8), CNC γ (9), NO (11) and N₂H₄ (12)] and [Fe(NO)(Et₂NpyS₄)]BF₄ (10). Protonation or alkylation of the thiolate donor atoms resulted in a series of complexes

[Fe(CO)(Et₂NpyS₄-R)]BF₄ [R = H (8a), Et (8b)] and [Fe(CO)(Et₂NpyS₄-Et₂)](BF₄)₂ (8c) but no labilisation of the Fe-CO bond was observed. Only in complex 8 could the CO coligand be exchanged by NO⁺ to give [Fe(NO)(Et₂NpyS₄)]BF₄ (10). Reduction of 10 using N₂H₄, NH₃ or N₃⁻ afforded the 19 valence electron species [Fe(NO)(Et₂NpyS₄)] (11). [Ru(NO)(Et₂NpyS₄)]Br (13) was synthesised by template alkylation of Bu₄N[Ru(NO)(S₂C₆H₄)₂] using Et₂Npy(CH₂Br)₂ (3). Under reducing conditions, 13 releases the NO coligand to give [[Ru(Et₂NpyS₄)]₂] (14), while in the presence of N₂H₄, [Ru(N₂H₄)(Et₂NpyS₄)] (15) was formed. The complexes were well characterised including the solid-state structures in most cases. X-ray structural analyses of 7, 8, 9, 10, 12 and 15 revealed that all complexes exhibit *trans*-thiolate donors irrespective of the σ - π - or σ -ligand character of L. (© Wiley-VCH Verlag GmbH & Co. KGaA, 69451 Weinheim, Germany, 2004)

Introduction

Transition metals in sulfur-dominated coordination spheres form the active centres of numerous oxidoreductases such as nitrogenases, hydrogenases and CO dehydrogenases.^[1] In the search for low-molecular weight compounds that combine structural and reactivity features of these [MS] enzymes, we have found that transition metal complexes containing [M(pyS₄)] fragments [pyS₄²⁻ = 2,6-bis(2-mercaptophenylthiomethyl)pyridine(2-)] (M = Fe, Ru) bind many nitrogenase-relevant molecules such as CO, NO, N₂H₄, N₂H₂ and NH₃, although not N₂ (Scheme 1).^[2]



Scheme 1. Schematic structures of RpyS₄-H₂ ligands and [M(RpyS₄)] fragments (M = Fe, Ru; R = H, Et₂N)

As was pointed out earlier,^[3] and even more so for the syntheses of the first pair of mono- and dinuclear N₂ complexes [Ru(N₂)(P*i*Pr₃)(N₂Me₂S₂)]^[4] and [μ-N₂{Ru(P*i*Pr₃)(N₂Me₂S₂)}₂]^[5] [N₂Me₂S₂²⁻ = *N,N'*-dimethyl-1,2-ethanediamine-*N,N'*-bis(2-benzenethiolate)(2-)] which formed directly from N₂ and sulfur-metal complex fragments under mild conditions, a major factor for the binding of N₂ can be considered to be a high electron density at the metal centres. Although the position of the ν(CO) bands in [Fe(CO)(pyS₄)] (1963 cm⁻¹)^[6] and [Ru(CO)(pyS₄)] (1954 cm⁻¹)^[2g] indicate a relatively high electron density at the metal centres, no N₂ complexes could be obtained. It is possible that the electron density is not high enough to enable

[†] Transition Metal Complexes with Sulfur Ligands, 166. Part 165: D. Sellmann, K. Hein, F. W. Heinemann, *Inorg. Chem. Acta* **2004**, 357, 3739–3745.

[a] Institut für Anorganische Chemie der Universität Erlangen-Nürnberg, Egerlandstraße 1, 91058 Erlangen, Germany Fax: (internat.) + 49-9131-8527367

E-mail: shaban@anorganik.chemie.uni-erlangen.de

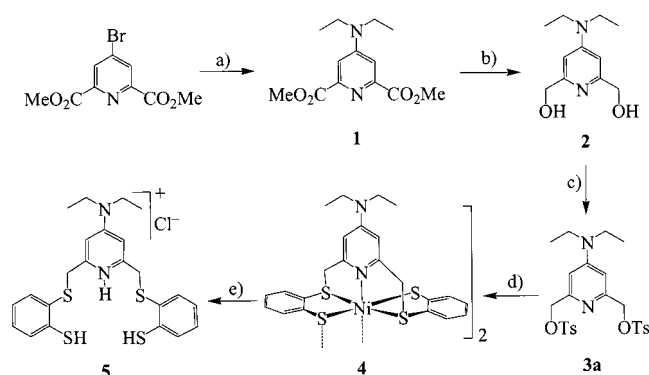
[†] Deceased.

the coordination of N_2 . Numerous efforts have been made to increase the electron density in $[M(\text{pyS}_4)]$ fragments by modifying the benzene ring substituents with electron-donating groups but these have remained unsuccessful.^[2d,6] Apparently, the electronic changes in the benzene rings are not transmitted beyond the sulfur donor atoms to the metal centres. These findings prompted us to start a systematic study of the influence of the pyridine ring substituents on the electron density at the metal centres and the reactivity of the resultant complexes. We describe herein the syntheses of the new $\text{Et}_2\text{NpyS}_4\text{-H}_2$ ligand and some related iron and ruthenium complexes. The similarities and differences between $[M(\text{Et}_2\text{NpyS}_4)]$ and $[M(\text{pyS}_4)]$ complexes ($M = \text{Ru}$ and Fe) are discussed in detail.

Results and Discussions

Synthesis of the New Ligand $\text{Et}_2\text{NpyS}_4\text{-H}_2$

The target ligand $\text{Et}_2\text{NpyS}_4\text{-H}_2\cdot\text{HCl}$ (**5**) was synthesised according to the route indicated in Scheme 2.

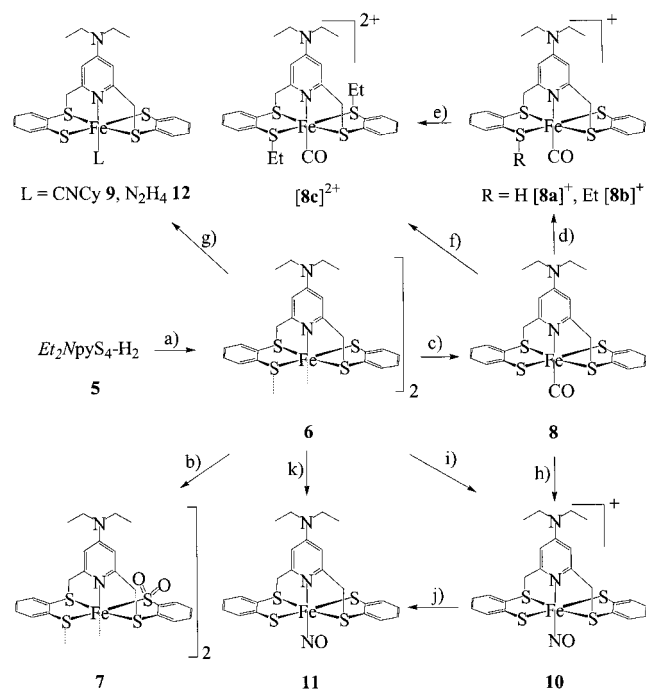


Scheme 2. Synthesis of the target $\text{Et}_2\text{NpyS}_4\text{-H}_2\cdot\text{HCl}$ ligand **5**: a) + Et_2NH , K_2CO_3 , DMSO, 55°C ; b) + NaBH_4 , EtOH, reflux, 16 h; c) + tosyl chloride, KOH, THF; d) + $\text{Na}_2[\text{Ni}(\text{S}_2\text{C}_6\text{H}_4)_2]$, THF, MeOH, 60°C , 2 h; e) HCl_{aq} , CH_2Cl_2

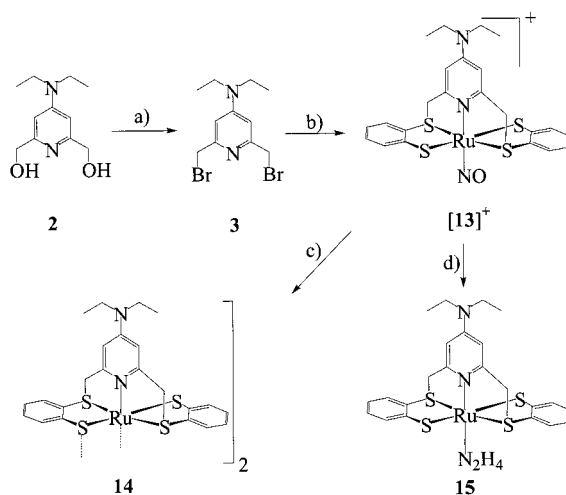
Treatment of dimethyl 4-bromopyridine-2,6-dicarboxylate^[7] with excess Et_2NH and K_2CO_3 in DMSO at 55°C for 28 h afforded dimethyl 4-(diethylamino)pyridine-2,6-dicarboxylate (**1**). The resultant ester **1** was reduced with NaBH_4 and continuously extracted with CHCl_3 at 45°C for 72 h to yield 4-(diethylamino)-2,6-bis(hydroxymethyl)pyridine (**2**). Treatment of **2** with either HBr or tosyl chloride afforded 2,6-bis(bromomethyl)-4-(diethylamino)pyridine (**3**) or 4-(diethylamino)-2,6-bis(tosyloxymethyl)pyridine (**3a**), respectively. Compound **3a** was subsequently used for the template alkylation of $[\text{Ni}(\text{S}_2\text{C}_6\text{H}_4)_2]^{2-}$ ^[8] to give $[\{\text{Ni}(\text{Et}_2\text{NpyS}_4)\}_x]$ (**4**). Complex **4** is paramagnetic with μ_{eff} (293 K) = $2.25 \mu_{\text{B}}$ which is consistent with two unpaired electrons per Ni centre. A solution of **4** in CH_2Cl_2 was readily hydrolysed when treated with aqueous concentrated HCl to afford $\text{Et}_2\text{NpyS}_4\text{-H}_2$ as its HCl salt.

Syntheses and Reactions of Complexes

Schemes 3 and 4 summarise the syntheses and reactions of $\text{Et}_2\text{NpyS}_4^{2-}$ complexes.



Scheme 3. Synthesis and reactions of iron complexes: a) + $\text{FeCl}_2\cdot 4\text{H}_2\text{O}$, THF, room temp.; b) + air, CHCl_3 , 72 h; c) + CO, THF, room temp.; d) + HBF_4 , CH_2Cl_2 , -78°C or Et_3OBF_4 , room temp.; e) + Et_3OBF_4 , CH_2Cl_2 ; f) 2 Et_3OBF_4 , CH_2Cl_2 ; g) + L (CNCy or N_2H_4)/THF; h) + NOBF_4 , CH_2Cl_2 , 0°C ; room temp.; i) + NOBF_4 , CH_2Cl_2 , room temp.; j) + N_2H_4 , MeOH or DMF; k) NO, CH_2Cl_2 .



Scheme 4. Synthesis and reactions of ruthenium complexes: a) + $\text{HBr}/\text{H}_2\text{O}$, reflux, 16 h; b) + $\text{Bu}_4\text{N}[\text{Ru}(\text{NO})(\text{S}_2\text{C}_6\text{H}_4)_2]$, THF, 60°C , 2 h; c) + NH_3 , MeOH, 1 h; d) + N_2H_4 , THF, 2 h, room temp.

The reaction between $\text{FeCl}_2\cdot 4\text{H}_2\text{O}$ and the $\text{Et}_2\text{NpyS}_4^{2-}$ anion resulting from deprotonation of **5** with 3 equiv. of LiOMe afforded yellow paramagnetic $[\{\text{Fe}(\text{Et}_2\text{NpyS}_4)\}_x]$ (**6**) [μ_{eff} (293 K) = $5.15 \mu_{\text{B}}$]. The solid-state structure of **6** has not yet been determined. However, x is probably 2. Aer-

ial oxidation of **6** afforded the sulfinato complex [$\{\text{Fe}(\text{Et}_2\text{NpyS}_4-\text{O}_2)\}_2$] (**7**) showing $\nu_a(\text{SO}_2)$ and $\nu_s(\text{SO}_2)$ IR (KBr) bands at 1238, 1185, 1133 and 983 cm⁻¹.^[9] An X-ray structure determination established that **7** is dinuclear and exhibits a *trans*-thiolate structure. A possible reason for this mild thiolate oxidation could be the high basicity of the thiolate donors originating from the presence of the Et₂N substituent. Dinuclear **6** readily coordinates CO or CNCy to give the C₂-symmetric and diamagnetic mononuclear complexes [Fe(CO)(Et₂NpyS₄)] (**8**) and [Fe(CNCy)(Et₂NpyS₄)] (**9**), respectively, indicating that **6** partially dissociates in solution into two unsaturated monomers. Complexes **8** and **9** exhibit characteristic $\nu(\text{CO})$ (1948 cm⁻¹) and $\nu(\text{CNCy})$ (2105 cm⁻¹) bands in their IR (KBr) spectra. The $\nu(\text{CO})$ of **8** is low when compared with that of [Fe(CO)(pyS₄)] (1963 cm⁻¹),^[6] indicating a high electron density at the Fe centre which in turn results in a strong Fe-CO bond. Complex **8** could also be obtained directly from FeCl₂·4H₂O and Et₂NpyS₄²⁻ in the presence of CO.

During attempts to diminish the inertness of [Fe(CO)(Et₂NpyS₄)] (**8**) towards substitution, the thiolate donor atoms were protonated or alkylated using either HBF₄ or Et₃OBF₄, affording the thioether derivatives [Fe(CO)(Et₂NpyS₄-R)]BF₄ [R = H (**8a**), Et (**8b**)] and [Fe(CO)(Et₂NpyS₄-Et₂)](BF₄)₂ (**8c**). Complexes **8a-c** were completely characterised and each shows a characteristic $\nu(\text{CO})$ band in the 1975–2016 cm⁻¹ range but they proved as inert towards substitution as their precursor **8**. For example, **8a** is deprotonated in solvents such as Et₂O, H₂O, MeOH, DMF or THF to regenerate **8** indicating that the protonation is reversible and does not lead to CO cleavage. This is in contrast to the parent complex [Fe(CO)(pyS₄-H)]BF₄, in which the CO ligand is labile and undergoes elimination to give [$\{\text{Fe}(\text{pyS}_4-\text{H})\}_2$](BF₄)₂.^[6] One possible reason for the stability of the Fe-CO bond in **8a** may be the higher electron density at the iron centre. A comparison of the $\nu(\text{CO})$ bands (in KBr) of [Fe(CO)(Et₂NpyS₄-H)]BF₄ (**8a**) and [Fe(CO)(pyS₄-H)]BF₄ (1975 cm⁻¹ vs. 1996 cm⁻¹)^[6] shows that the iron centres in the [Fe(Et₂NpyS₄)] fragments have a higher electron density than in the [Fe(pyS₄)] fragments, thus favouring bonding of the good π -acceptor CO. The low $\nu(\text{CO})$ frequency of **8** prompted us to attempt to obtain an [Fe(Et₂NpyS₄)] dinitrogen complex. For this purpose, a solution of **8** was UV-irradiated under N₂ for a prolonged period of time at different temperatures. However, the CO coligand dissociated and dinuclear **6** formed. Complex **8** was found to react only with NOBF₄ at 0 °C to afford the 18 valence electron (VE) complex [Fe(NO)(Et₂NpyS₄)]BF₄ (**10**). Complex **10** could also be obtained directly from **6** and NOBF₄.

The relatively high $\nu(\text{NO})$ frequency of **10** (1882 cm⁻¹ in KBr) made the [10]⁺ cation a candidate for attempts to convert the NO into an N₂ ligand by addition of nitrogen nucleophiles to the nitrosyl N atom.^[10] For this purpose, **10** was treated with NH₃, N₂H₄ or N₃⁻. However, in none of these cases did a nucleophilic addition to the NO coligand take place and, rather, the nucleophiles acted as reductants

yielding the neutral 19 VE complex [Fe(NO)(Et₂NpyS₄)] (**11**), showing a $\nu(\text{NO})$ band at 1637 cm⁻¹ in its IR (KBr) spectrum. Subsequent experiments revealed that even N₂H₄ or solvents such as MeOH or DMF could reduce the cationic [10]⁺ to give neutral **11**. Alternatively, **11** could be synthesised directly from **6** and an equimolar amount of NO gas. Complex **11** is highly reactive and can be oxidised to give the [10]⁺ cation.

Treatment of an equimolar amount of **6** with N₂H₄ afforded the hydrazine complex [Fe(N₂H₄)(Et₂NpyS₄)] (**12**). Complex **12** is stable and could be isolated as a solid and completely characterised. This is in contrast to the analogous [Fe(N₂H₄)(pyS₄)]^[2a] which is highly labile towards N₂H₄ elimination and could be isolated in crystalline form only in the presence of excess N₂H₄. One possible reason for this high stability could be that all N₂H₄ hydrogen atoms are involved in both intra- and intermolecular hydrogen bonding as found for solid **12** in the solid state.

The unsuccessful attempts to obtain an [Fe(Et₂NpyS₄)] dinitrogen complex prompted us to also study ruthenium complexes which could be expected to be less labile (Scheme 4).

As a first target complex [Ru(NO)(Et₂NpyS₄)]Br (**13**) was prepared. It was obtained by template alkylation of Bu₄N-[Ru(NO)(S₂C₆H₄)₂]^[11] with Et₂Npy(CH₂Br)₂ (**3**) in boiling THF. Complex **13** exhibits a low $\nu(\text{NO})$ frequency (1858 cm⁻¹ in KBr) compared with the related complex [Ru(NO)(pyS₄)]Tos (1892 cm⁻¹).^[2e] This again indicates a higher electron density at the ruthenium centre. Attempts to obtain an [Ru(Et₂NpyS₄)] dinitrogen complex from the reaction of **13** with NH₃ in MeOH resulted in the formation of the thiolate bridged dinuclear [$\{\text{Ru}(\text{Et}_2\text{NpyS}_4)\}_2$] (**14**). Monitoring of the reaction by solution IR spectroscopy showed that at first **13** [$\nu(\text{NO}) = 1880 \text{ cm}^{-1}$ in MeOH] is reduced to give the 19 VE electron species [Ru(NO)(Et₂NpyS₄)] [$\nu(\text{NO}) = 1640 \text{ cm}^{-1}$ in MeOH]^[2b] which is highly labile and releases NO to give dinuclear **14**. Complex **14** is practically insoluble in all common solvents and inert towards cleavage reactions. When a red brown THF suspension of **13** was treated with N₂H₄, a green solution was formed from which the hydrazine complex [Ru(N₂H₄)(Et₂NpyS₄)] (**15**) was isolated. Complex **15** is stable over prolonged periods of time in both the solid state and solution.

Characterization and General Properties of the Complexes

As far as possible, all complexes have been characterised by common spectroscopic methods and elemental analyses and, with the exception of **6** and **11**, they are all diamagnetic. All complexes, except the dinuclear species **6** proved to be soluble in THF, CH₂Cl₂ and DMF. The IR (KBr) spectra show a typical pattern for the [M(Et₂NpyS₄)] fragment besides the characteristic bands of the coligands. For example, the $\nu(\text{CNCy})$ band at 2105 cm⁻¹ indicates coordination of the CNCy ligand in **9**. Characteristic strong $\nu(\text{CO})$ bands were observed for **8** (1948 cm⁻¹), **8a** (1974 cm⁻¹), **8b** (1980 cm⁻¹) and **8c** (2007 cm⁻¹), while weak $\nu(\text{N-H})$ bands at 3318, 3285 and 3237, and 3318, 3242 and

3100 cm^{-1} appeared for the hydrazine complexes **12** and **15**, respectively. Strong $\nu(\text{NO})$ bands at 1882, 1637 and 1858 cm^{-1} characterise the nitrosyl complexes **10**, **11** and **13**, respectively.

The mass spectra in all cases exhibited peaks corresponding to either the molecular ion or ions resulting from loss of the coligands. The $^{13}\text{C}\{^1\text{H}\}$ NMR spectra proved particularly helpful in establishing the diastereomeric purity of the complexes and the twofold symmetry of the $[\text{M}(\text{Et}_2\text{NpyS}_4)]$ fragments. ^1H and $^{13}\text{C}\{^1\text{H}\}$ NMR spectra corroborated the C_2 symmetry of complexes **8**, **8c**, **9**, **10**, **12**, **13** and **15**, and the C_1 symmetry of complex **8b**. The hydrazine complex **12** gave rise to a broad singlet at $\delta = 2.9$ ppm which can be attributed to *Fe*-bound and terminal NH_2 groups, while **15** gave rise to two doublets at $\delta = 4.2$ and 4.4 ppm which can be attributed to an *Ru*-bound NH_2 group and a multiplet at $\delta = 3.3$ ppm which can be assigned to the terminal NH_2 group.

Benzene and Pyridine Ring Substituent Effects

In the search for complexes which exhibit electron-rich metal centres, we have found that the benzene ring substituents have no significant influence on the electron density at the metal centres. In other words, the electronic changes in the benzene rings cannot be transmitted beyond the sulfur donors to the metal centres.^[6,12] The $\nu(\text{CO})$ or $\nu(\text{NO})$ frequencies which sensitively reflect electronic changes at the metal centres are practically identical in the corresponding complexes (Table 1). It was therefore of interest to examine whether such an electron-donating effect of the pyridine ring Et_2N substituent would reach and be detectable at the metal centres of the homologous complexes.

Table 1. The $\nu(\text{CO})$ and $\nu(\text{NO})$ frequencies of $[\text{Fe}(\text{NS}_4)]$ cores with electron-donating benzene and pyridine ring substituents

Complex	$\nu(\text{CO})$ ^[a]	Complex	$\nu(\text{NO})$ ^[a]
$[\text{Fe}(\text{CO})(\text{pyS}_4)]$	1963 ^[6]	$[\text{Fe}(\text{NO})(\text{pyS}_4)]^+$	1893 ^[6]
$[\text{Fe}(\text{CO})(\text{pybuS}_4)]$	1969 ^[6]	$[\text{Fe}(\text{NO})(\text{Et}_2\text{NpyS}_4)]^+$ (10)	1882 ^[b]
$[\text{Fe}(\text{CO})(\text{Et}_2\text{NpyS}_4)]$ (8)	1948 ^[b]	$[\text{Fe}(\text{NO})(\text{pyS}_4)]$	1648 ^[6]
		$[\text{Fe}(\text{NO})(\text{Et}_2\text{NpyS}_4)]$ (11)	1637 ^[b]

^[a] In KBr [cm^{-1}]. ^[b] This work.

Table 1 demonstrates that all iron complexes with $[\text{Fe}(\text{Et}_2\text{NpyS}_4)]$ cores show significant shifts of the $\nu(\text{CO})$ and $\nu(\text{NO})$ bands to lower wave numbers by about 11–22 cm^{-1} indicating that the electron donation of the pyridine

ring substituents increases the electron density. This conclusion is supported by the high basicity of the sulfur donor atoms which form strong hydrogen bonds as found in the solid-state structures of **12**, **15** and **15**· N_2H_4 . Further supporting observations include the cyclic voltammograms of the isoelectronic iron complexes $[\text{Fe}(\text{CO})(\text{Et}_2\text{NpyS}_4)]$ (**8**) and $[\text{Fe}(\text{CO})(\text{pyS}_4)]$ ^[6] as well as the nitrosylruthenium complexes $[\text{Ru}(\text{NO})(\text{Et}_2\text{NpyS}_4)]\text{Br}$ (**13**) and $[\text{Ru}(\text{NO})(\text{Et}_2\text{NpyS}_4)]\text{Tos}$ ^[2e] (Figure 1, Table 2). A comparison of the redox potentials of the carbonyliron complexes $[\text{Fe}(\text{CO})(\text{Et}_2\text{NpyS}_4)]$ (**8**) and $[\text{Fe}(\text{CO})(\text{pyS}_4)]$ ^[6] (+361 mV vs. +514 mV in CH_2Cl_2) indicates the electron-donating nature of the Et_2N substituent which makes oxidation easier. On the other hand, the redox potentials of the nitrosylruthenium cations $[\text{Ru}(\text{NO})(\text{Et}_2\text{NpyS}_4)]^+$ (**13**) and $[\text{Ru}(\text{NO})(\text{Et}_2\text{NpyS}_4)]$ ^[2e] (−467, −1524 mV vs. −275, −1200 mV in DMF) indicate that the Et_2N substituent renders cationic complexes with $[\text{Fe}(\text{Et}_2\text{NpyS}_4)]$ fragments more difficult to reduce. Keeping all these observations in mind, we can conclude that the Et_2N substituent has a significant influence on the electron density in $[\text{M}(\text{Et}_2\text{NpyS}_4)]$ cores.

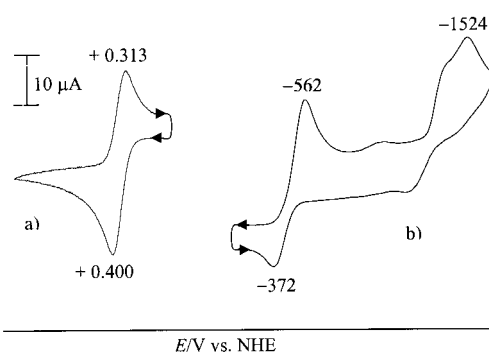


Figure 1. Cyclic voltammograms of a) $[\text{Fe}(\text{CO})(\text{Et}_2\text{NpyS}_4)]$ (**8**) in CH_2Cl_2 , b) $[\text{Ru}(\text{NO})(\text{Et}_2\text{NpyS}_4)]\text{Br}$ (**13**) in DMF (10^{-3} M, 10^{-1} Bu₄NPF₆, $\nu = 50$ mV/s, potentials given in mV)

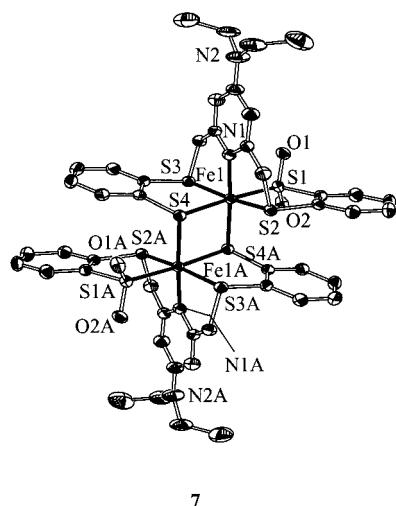
X-ray Crystal Structure Determinations

The crystal structures of the complexes $\{[\text{Fe}(\text{Et}_2\text{NpyS}_4 - \text{O}_2)]_2\} \cdot 8\text{CDCl}_3$ (**7**· 8CDCl_3), $[\text{Fe}(\text{CO})(\text{Et}_2\text{NpyS}_4)] \cdot \text{CDCl}_3$ (**8**· CDCl_3), $[\text{Fe}(\text{CNCy})(\text{Et}_2\text{NpyS}_4)] \cdot 2\text{THF}$ (**9**· 2THF), $[\text{Fe}(\text{NO})(\text{Et}_2\text{NpyS}_4)]\text{BF}_4 \cdot \text{CH}_2\text{Cl}_2$ (**10**· CH_2Cl_2), $[\text{Fe}(\text{N}_2\text{H}_4)(\text{Et}_2\text{NpyS}_4)]$ (**12**), $[\text{Ru}(\text{N}_2\text{H}_4)(\text{Et}_2\text{NpyS}_4)]$ (**15**) and $[\text{Ru}(\text{N}_2\text{H}_4)(\text{Et}_2\text{NpyS}_4)] \cdot \text{N}_2\text{H}_4$ (**15**· N_2H_4) were determined by X-ray crystallography. Figures 2–4 depict the molecular structures of the complexes. Tables 3 and 4 list selected bond lengths and angles.

Table 2. Redox potentials of carbonyl and nitrosyl complexes with $[\text{M}(\text{NS}_4)]$ cores

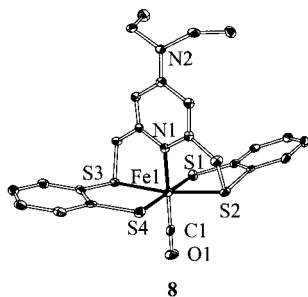
Complex	Redox potentials in CH_2Cl_2 [mV] ^[a]	Complex	Redox potentials in DMF [mV] ^[a]
$[\text{Fe}(\text{CO})(\text{pyS}_4)]$	+ 514 ^[6]	$[\text{Ru}(\text{NO})(\text{pyS}_4)]^+$	− 275, − 1200 ^[2e]
$[\text{Fe}(\text{CO})(\text{Et}_2\text{NpyS}_4)]$ (8)	+ 361 ^[b]	$[\text{Ru}(\text{NO})(\text{Et}_2\text{NpyS}_4)]^+$ (13)	− 467, − 1524 ^[b]

^[a] Related to NHE. ^[b] This work.

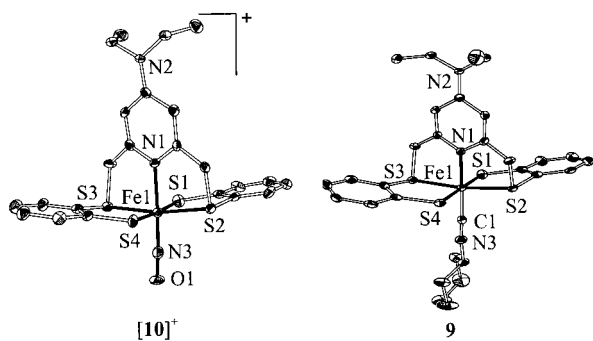


7

Figure 2. Molecular structure of [Fe(Et₂NpyS₄-O₂)]₂·8CHCl₃ (7·8CHCl₃) (50% probability ellipsoids, all solvate molecules, anions and C-bound H atoms omitted)



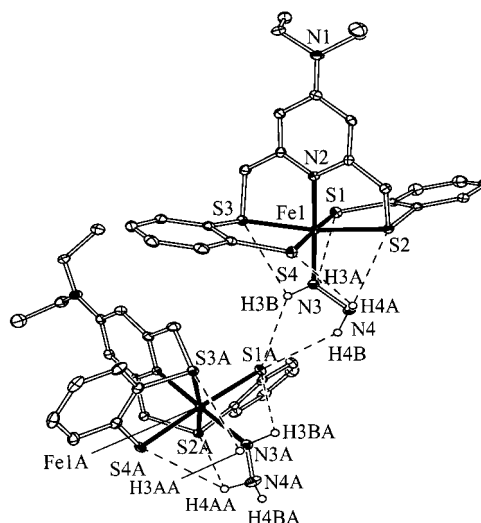
8

[10]⁺

9

Figure 3. Molecular structures of [Fe(CO)(Et₂NpyS₄)]·CDCl₃ (8·CDCl₃), [Fe(CNCy)(Et₂NpyS₄)]·2THF (9·2THF) and [Fe(NO)(Et₂NpyS₄)]BF₄·CH₂Cl₂ (10·CH₂Cl₂) (50% probability ellipsoids, all solvate molecules, anions and C-bound H atoms omitted)

The Et₂NpyS₄ ligand acts as a square-pyramidal coordination cap and the overall geometry around the iron centre is pseudo-octahedral. The pyridine N1 donor and the coligand L or the bridging S donor of a second Fe fragment as well as the two thiolate and the two thioether donor atoms of the Et₂NpyS₄²⁻ ligand occupy corresponding *trans* positions and thus provide the steric rigidity of the py(CH₂)₂ backbone. A comparison of the geometrical parameters of 8·CDCl₃, 9·2THF and 10·CH₂Cl₂ demonstrates that the Fe-donor distances in all cases lie in the usual



12

Figure 4. Molecular structure and hydrogen bonds (dashed lines) observed for [Fe(N₂H₄)(Et₂NpyS₄)] (12) (50% probability ellipsoids, C-bound H atoms omitted)

Table 3. Selected bond lengths [pm] and angles [°] for [Fe(Et₂NpyS₄-O₂)]₂·8CDCl₃ (7·8CDCl₃), [Fe(CO)(Et₂NpyS₄)]·CDCl₃ (8·CDCl₃), [Fe(CNCy)(Et₂NpyS₄)]·2THF (9·2THF), [Fe(NO)(Et₂NpyS₄)]BF₄·CH₂Cl₂ (10·CH₂Cl₂) and [Fe(N₂H₄)(Et₂NpyS₄)] (12)

	7·8CDCl ₃	8·CDCl ₃	9·2THF	10·CH ₂ Cl ₂	12
Fe(1)–N(1)	198.8(3)	201.5(2)	200.9(4)	199.2(4)	197.1(2)
Fe(1)–S(1)	218.8(2)	231.3(9)	231.1(2)	230.6(2)	230.46(6)
Fe(1)–S(2)	221.6(2)	224.0(1)	221.9(2)	224.9(2)	222.78(5)
Fe(1)–S(3)	223.3(2)	222.7(1)	221.6(2)	224.5(2)	223.22(6)
Fe(1)–S(4)	229.9(2)	229.8(1)	230.6(2)	231.3(2)	229.42(5)
Fe(1)–L	233.4(2)	176.5(3)	183.4(5)	163.8(5)	203.73(2)
N(1)–Fe(1)–S(1)	89.7(1)	91.42(7)	89.8(2)	88.3(2)	90.73(5)
N(1)–Fe(1)–S(2)	86.1(2)	83.33(7)	84.7(2)	85.1(2)	84.59(5)
N(1)–Fe(1)–S(3)	84.8(2)	84.34(7)	84.7(2)	85.0(2)	85.26(5)
N(1)–Fe(1)–S(4)	93.1(1)	89.32(7)	90.8(2)	87.6(2)	92.08(5)
N(1)–Fe(1)–L	176.8(1)	178.9(2)	178.6(2)	177.4(2)	178.59(7)

range observed for diamagnetic [FeNS₄] cores.^[2a,2b,2c,6] The Fe–S(thiolate) distances (average 230 pm) are slightly longer than the Fe–S(thioether) distances (average 223 pm).

In complex 7·8CDCl₃, the oxygenation causes a significant effect in the Fe–S(sulfinate) distance while the other Fe–S and Fe–N distances remain practically unchanged. The Fe–S(sulfinate) distance decreases by about 12 pm [218(2) pm for 7·8CDCl₃ vs. 230 pm (average) for 8·CDCl₃, 9·2THF and 12]. An explanation could be that the Fe–S distances are governed by three factors: 1) the σ-donor ability, expected to be best in the thiolate which decreases with increasing oxygenation, 2) a contraction in the size of the sulfur atoms as the formal oxidation state of the sulfur atoms changes from –2 (for Fe–S in complexes 8·CDCl₃, 9·2THF and 10) to +2 [for Fe–S(sulfinate) in complex 7·8CDCl₃], and 3) the destabilisation of the Fe–S bond due

Table 4. Selected bond lengths [pm] and angles [°] for [Ru(N₂H₄)(Et₂NpyS₄)] (**15**) and [Ru(N₂H₄)(Et₂NpyS₄)]·N₂H₄ (**15**·N₂H₄)

	15	15 ·N ₂ H ₄		15	15 ·N ₂ H ₄
Ru(1)–N(1)	205.6(3)	205.4(3)	N(1)–Ru(1)–S(1)	90.33(8)	90.54(9)
Ru(1)–S(1)	237.51(9)	239.2(2)	N(1)–Ru(1)–S(2)	83.21(8)	83.60(9)
Ru(1)–S(2)	230.49(9)	230.7(1)	N(1)–Ru(1)–S(3)	83.71(8)	84.29(9)
Ru(1)–S(3)	231.06(9)	228.6(1)	N(1)–Ru(1)–S(4)	91.81(8)	90.63(9)
Ru(1)–S(4)	237.23(9)	237.9(2)	N(1)–Ru(1)–N(3)	179.09(11)	176.6(2)
Ru(1)–N(3)	213.70(3)	213.7(4)	Ru(1)–N(3)–N(4)	115.90(2)	118.3(3)
N(3)–N(4)	146.40(4)	144.6(5)			
N(5)–N(6)	–	139.6(6)			

to a repulsive interaction between the filled d orbital of the metal atom and two lone pairs of the thiolate sulfur atom.^[9a,13]

The crystal structures of the complexes **12**, **15** and **15**·N₂H₄ deserve special interest because all types of hydrazine hydrogen atoms are involved in a system of inter- and intramolecular N–H···S and N–H···N hydrogen bonding with the sulfur donors (thiolate, thioether) as well as the solvate hydrazine N atoms. The hydrogen bonds are indicated by both the N–H···S and N–H···N vectors as well as the distances which are shorter than the sum of the corresponding van der Waals radii ($r_H = 120$ pm, $r_S = 185$ pm).^[14] Figure 3 shows the molecular structures and the hydrogen bonding geometry for **12** and **15**·N₂H₄. The parameters of the hydrogen bonds are collected in Table 5.

The crystal lattices of **12** and **15** contain chains of molecules which are connected by intermolecular N–H···S(thiolate) hydrogen bonds and each molecule exhibits additional intramolecular N–H···S hydrogen bonds. The type of bonds, bond lengths and bond angles in the two complexes are very similar, only **12** contains an additional N–H···S bond. The crystal lattice of **15**·N₂H₄ additionally contains intermolecular N–H···N hydrogen bonds between the solvate hydrazine and the coordinated hydrazine. This system of hydrogen bonds is of interest because it contributes significantly to the stabilisation of the N₂H₄ coligand

and a similar effect may stabilise the intermediate diazene complex which is assumed to be essential for N₂ fixation.^[2c]

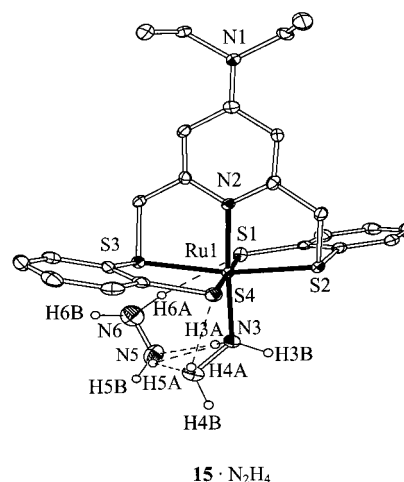


Figure 5. Molecular structure and hydrogen bonds (dashed lines) observed for [Ru(N₂H₄)(Et₂NpyS₄)]·N₂H₄ (**15**·N₂H₄) (50% probability ellipsoids, C-bound H atoms omitted)

Conclusion

The new pentadentate Et₂NpyS₄–H₂ ligand has been synthesised with the aim of preparing transition metal com-

Table 5. Hydrogen bond parameters [pm and °] for [Fe(N₂H₄)(Et₂NpyS₄)] (**12**), [Ru(N₂H₄)(Et₂NpyS₄)] (**15**) and [Ru(N₂H₄)(Et₂NpyS₄)]·N₂H₄ (**15**·N₂H₄)

D–H···A	<i>d</i> (D···A)		<i>d</i> (D–H)		<i>d</i> (H···A)		<i>v</i> (DHA)	
	12	15	12	15	12	15	12	15
N(3)–H(3A)···S(1A) ^[a]	344.1(2)	335.3(3)	89(3)	99	277(3)	260	134(2)	132
N(3)–H(3A)···S(3)	311(2)	–	89(3)	–	300(3)	–	88(2)	–
N(3)–H(3B)···S(1)	304.5(2)	316.8(3)	90(3)	82	268(3)	288	105(2)	103
N(4)–H(4A)···S(4)	348.1(2)	359.9(3)	88(3)	88	292(3)	301	123(2)	126
N(4)–H(4A)···S(2)	316.3(2)	327.7(3)	88(3)	88	285(3)	291	103(2)	107
N(4)–H(4B)···S(1A) ^[a]	340.1(2)	337.3(3)	88(3)	83	265(3)	266	144(2)	145
15 ·N ₂ H ₄								
N(3)–H(3A)···N(5)	323.6(6)	–	102	–	227	–	157	–
N(4)–H(4A)···S(1)	337.2(4)	–	104	–	256	–	135	–
N(5)–H(5A)···N(4)	314.9(6)	–	106	–	218	–	151	–
N(5)–H(5A)···N(3)	323.6(6)	–	106	–	259	–	119	–
N(6)–H(6A)···S(4)	366.7(5)	–	105	–	264	–	157	–

^[a] Symmetry transformations used to generate equivalent atoms: $x + 1/2, y, -z - 1/2$.

plexes which exhibit electron-rich metal centres, possess a core configuration with thiolate, thioether and amine donors related to the structure of [M(pyS₄)] fragments (M = Fe and Ru), and bind biologically relevant small molecules. This goal was achieved as evidenced by the low $\nu(\text{CO})$ frequency of [Fe(CO)(Et₂NpyS₄)] (1948 cm⁻¹) compared with the analogous [Fe(CO)(pyS₄)] (1963 cm⁻¹). The [M(Et₂NpyS₄)] fragments (M = Fe, Ru) were found to bind and stabilise many nitrogenase-relevant molecules such as CO, NO, NO⁺, CNCy and N₂H₄. The results also revealed that the Et₂N substituent not only increases the electron density at the metal centres but also at the sulfur donor atoms which leads to highly basic sulfur donors. This high basicity influences the reactivity of the M-L bonds. For example, the protonated complex [Fe(CO)(Et₂NpyS₄-H)]-BF₄ is deprotonated only in solution to give [Fe(CO)(Et₂NpyS₄)], while the related complex [Fe(CO)(pyS₄-H)]BF₄ is labile and undergoes CO elimination to give [Fe(pyS₄-H)]₂(BF₄).

The X-ray structural analyses of [Fe(N₂H₄)(Et₂NpyS₄)] and [Ru(N₂H₄)(Et₂NpyS₄)] revealed that such complexes can form intra- and intermolecular N-H...S and N-H...N hydrogen bonds. This stabilises the hydrazine complex [Fe(N₂H₄)(Et₂NpyS₄)] and makes it isolable and stable in the solid state. This is in contrast to the parent complex [Fe(N₂H₄)(pyS₄)] which was highly labile with respect to elimination of the N₂H₄ coligand and could not be isolated.

Experimental Section

General: Unless noted otherwise, all procedures were carried out under nitrogen using Schlenk techniques. Stringently dried solvents were used. As far as possible, reactions were monitored by IR or NMR spectroscopy. Spectra were recorded with the following instruments: IR (KBr discs or CaF₂ corvettes, solvent bands were compensated): Perkin-Elmer 983, 1620 FT-IR, and 16PC FT-IR. NMR: Jeol-JNM-GX 270, EX 270, and Lambda LA 400 with the proton solvent signals used as an internal reference. Spectra were recorded at 25 °C. MS: Jeol MSTATION 700 spectrometer. Elemental analyses: Carlo Erba EA 1106 or 1108 analyser. Magnetic susceptibility: Johnson Matthey susceptibility balance. Cyclic voltammograms were recorded using an EG&G potentiostat PAR model 264A and a conventional three-electrode configuration consisting of a glassy carbon working electrode, a platinum auxiliary electrode and a platinum reference electrode. Ferrocene was used as an internal reference, $E(\text{Fc}/\text{Fc}^+) = +400$ mV (vs. NHE).^[15] The reversibility of the voltammograms and the number of electrons involved in the redox processes at 25 °C were determined as described in the literature.^[16] "S₂"-H₂ (1,2-benzenedithiol),^[17] dimethyl 4-bromo-pyridine-2,6-dicarboxylate^[7] and Bu₄N[Ru(NO)(S₂C₆H₄)₂]^[11] were prepared as described in the literature. Anhydrous hydrazine was obtained by twofold distillation of N₂H₄·H₂O from KOH under reduced pressure.

Et₂Npy(CO₂Me)₂ (1): Anhydrous K₂CO₃ (4.15 g, 30 mmol) and diethylamine (20 mL, 192.5 mmol) were added to a white suspension of dimethyl 4-bromo-pyridine-2,6-dicarboxylate (6.89 g, 25.1 mmol) in DMSO (200 mL). The resultant yellow-brown mixture was heated at 55–60 °C for 48 h. The resultant orange-brown

suspension was cooled to room temperature and poured onto ice-cold water (250 mL). A yellow solid formed which was separated by filtration, washed with water and dried in vacuo. Yield: 6.32 g of **1** (34%). ¹H NMR (CDCl₃, 269.60 MHz): $\delta = 1.20$ (t, 6 H, 2CH₂CH₃), 3.44 (q, 4 H, 2CH₂CH₃), 3.95 (s, 6 H, 2COOCH₃), 7.45 (s, 2 H, H _{β} , pyridine) ppm. IR (KBr): $\tilde{\nu} = 1748, 1708$, (vs, C=O) cm⁻¹. MS (FD⁺, CHCl₃): $m/z = 266$ [M⁺]. C₁₃H₁₈N₂O₄ (266.29): calcd. C 58.63, H 6.81, N 10.52; found C 58.44, H 6.92, N 10.37.

Et₂Npy(CH₂OH)₂ (2): NaBH₄ (2.96 g, 40 mmol) was added portionwise to **1** (4.05 g, 16 mmol) in ethanol (200 mL). The mixture was kept at room temperature for 1.5 h and was then heated to reflux for 16 h. The solvent was evaporated, the residue treated with a saturated solution of NaHCO₃ (50 mL) and heated to reflux for 1.5 h. H₂O (100 mL) was added and the aqueous phase was extracted continuously with CHCl₃ (500 mL) over 2 d. The CHCl₃ was evaporated to give a colourless solid. Yield 2.83 g of **2** (88%). ¹H NMR ([D₆]DMSO, 269.60 MHz): $\delta = 1.10$ (t, ³J_{H,H} = 7.1 Hz, 6 H, CH₂CH₃), 3.33 (q, 4 H, CH₂CH₃), 4.35 (d, ²J_{H,H} = 5.5 Hz, 4 H, 2CH₂), 5.14 (t, ³J_{H,H} = 5.8 Hz, 2 H, 2OH), 6.51 (s, 2 H, H _{β} pyridine) ppm. MS (FD, DMSO): $m/z = 210$ [M⁺].

Et₂Npy(CH₂Br)₂ (3): A solution of **2** (400 mg, 1.9 mmol) in 40% aqueous HBr (50 mL) was heated to reflux for 16 h. The aqueous phase was extracted with CHCl₃ (3 × 100 mL). The CHCl₃ extract was dried with MgSO₄ and the solvent removed in vacuo to give a white solid residue. Yield: 400 mg of **3**·0.16THF (62%). ¹H NMR (CDCl₃, 269.60 MHz): $\delta = 1.21$ (t, 6 H, 2CH₂CH₃), 3.41 (q, 4 H, 2CH₂CH₃), 4.50 (s, 4 H, 2CH₂), 6.55 (s, 2 H, H _{β} pyridine), ¹³C{¹H} NMR (CDCl₃, 67.83 MHz): $\delta = 12.27$ (CH₂CH₃), 33.43 (CH₂CH₃), 44.31 (CH₂Br), 105.24, 154.02, 156.01 [C(aryl)] ppm. IR (KBr): $\tilde{\nu} = 3033, 2969$ (m, C-H) cm⁻¹. FD MS: $m/z = 336$ [M]⁺. C_{11.7}H_{17.3}Br₂N₂O_{0.17} (348.10): calcd. C 40.26, H 5.02, N 8.05; found C 40.12, H 5.13, N 8.13.

[{Ni(Et₂NpyS₄)₂}] (4. a): A solution of **2**·0.75MeOH (1.17 g, 5.34 mmol) in THF (30 mL) was combined with KOH (0.9 g, 17.80 mmol) and cooled to 0 °C. Tosyl chloride (2.43 g, 10.68 mmol) in THF (20 mL) was added dropwise and the resultant suspension was stirred at 0 °C for 5 h and at room temperature for 14 h. The resultant solid was removed by filtration and washed with THF (30 mL). The washings and the filtrates were dried in vacuo, yielding a light brown viscous residue. Yield 2.6 g of Et₂Npy(CH₂-OTs)₂ (**3a**) (90%) which was used without further purification. **b):** Sodium (453 mg, 19.67 mmol) was dissolved in methanol (40 mL) and combined with 1,2-benzenedithiol (1.12 mL, 9.83 mmol) and a solution of Ni(ac)₂·4H₂O (1.22 g, 4.92 mmol) in MeOH (50 mL). Addition of Et₂Npy(CH₂OTs)₂ (**3a**) (2.55 g, 4.92 mmol) in THF (70 mL) to the dark-brown solution resulted in a brown precipitate which was isolated after 3 h, washed with THF and MeOH (30 mL each) and dried in vacuo. Yield: 2.0 g of [{Ni(Et₂NpyS₄)₂}]·1.5MeOH (**4**·1.5MeOH) (76%). IR (KBr): $\tilde{\nu} = 3050, 2968$, $\nu(\text{C-H})$ cm⁻¹. MS (FD⁺, MeOH): $m/z = 514$ [Ni(Et₂NpyS₄)₂]⁺, 1028 [{Ni(Et₂NpyS₄)₂}]⁺. C₂₃H₂₄N₂NiS₄ (515.40): calcd. C 52.22, H 5.36, N 5.00; found C 52.66, H 5.16, N 5.12. $\mu_{\text{eff}} = 2.25 \mu_{\text{B}}$ (297 K).

Et₂NpyS₄-H₂·HCl (5): Concentrated hydrochloric acid (15.14 mL) was added to a suspension of **4**·1.5MeOH (4.86 g, 9.60 mmol) in CH₂Cl₂ (200 mL) and the mixture was stirred for 30 min. The CH₂Cl₂ phase was separated from the aqueous green phase, dried with anhydrous Na₂SO₄ and the solvents were evaporated to dryness yielding a grey-green solid. Yield 1.7 g of **5**·2CH₃OH (32%). ¹H NMR (CD₂Cl₂, 269.60 MHz): $\delta = 0.94$ (t, ³J_{H,H} = 7.2 Hz, 6 H, 2CH₂CH₃), 3.14 (q, 4 H, 2CH₂CH₃), 4.38 (s, 2 H, 2SH), 4.40

(s, 4 H, 2CH₂), 5.92 (s, 2 H, H_β, pyridine), 7.04–7.38 (m, 8 H, C₆H₄), 7.78 (d, ²J_{H,H} = 6.5 Hz, 1 H, NH) ppm. IR (KBr): $\tilde{\nu}$ = 3414, 3255, 3070 (w, N–H), 2412 (w, S–H) cm⁻¹. MS (FD⁺, CH₂Cl₂): *m/z* = 495 [M]⁺. C₂₅H₃₅ClN₂O₂S₄ (559.3): calcd. C 53.69, H 6.31, N 5.01; found C 53.94, H 5.91, N 4.69.

[{Fe(Et₂NpyS₄)₂}] (6): Solid FeCl₂·4H₂O (77 mg, 0.39 mmol) was added to a light yellow solution of **5**·H₂O (220 mg, 0.39 mmol) and LiOMe (1.17 mL of a 1 M solution in MeOH) in THF (20 mL). A yellow precipitate resulted which was separated by filtration after 30 min, washed with THF (20 mL) and dried in vacuo. Yield: 105 mg of **6** (53%). IR (KBr): $\tilde{\nu}$ = 3050, 2966 (s, C–H) cm⁻¹. MS (FD⁺, DMF): *m/z* = 512 [Fe(Et₂NpyS₄)₂]⁺, 1024 [Fe(Et₂NpyS₄)₂]⁺. C₂₃H₂₄FeN₂S₄ (513.55): calcd. C 53.90 H 4.72, N 5.47, S 25.02; found C 53.65, H 5.11, N 5.46, S 24.86. μ_{eff} = 5.15 μ_{B} (297 K).

[{Fe(Et₂NpyS₄–O₂)₂}] (7): A yellow suspension of **6** (120 mg, 0.12 mmol) in CHCl₃ (30 mL) was stirred in air for 24 h. The resultant red-brown fine crystals were isolated, washed with CHCl₃ then H₂O (30 mL each) and dried in vacuo. Yield: 80 mg of 7·3CHCl₃·H₂O (23%). IR (KBr): $\tilde{\nu}$ = 2960 (s, C–H), 1238, 1185, 1133, 983 (s, SO₂) cm⁻¹. MS (FD⁺, CHCl₃): *m/z* = 512 [Fe(Et₂NpyS₄)₂]⁺, 1024 [Fe(Et₂NpyS₄)₂]⁺, 1088 [Fe(Et₂NpyS₄–O₂)₂]⁺. C₄₉H₅₅Cl₉Fe₂N₄O₅S₈ (1459.77): calcd. C 40.17, H 3.65, N 3.82, S 17.51; found C 40.12, H 4.09, N 3.84, S 17.85.

[Fe(CO)(Et₂NpyS₄)] (8): A stream of CO was passed through a yellow suspension of **6** (70 mg, 0.14 mmol) in THF (20 mL) for 10 min during the course of which a red solution formed which was kept under CO for a further 12 h, filtered and reduced in volume to about 2 mL. Addition of Et₂O (20 mL) precipitated a red solid which was separated by filtration and dried in vacuo. Yield 62 mg of **8**·0.7H₂O (84%). ¹H NMR (CD₂Cl₂, 269.60 MHz): δ = 1.06 (t, ³J_{H,H} = 7.05 Hz, 6 H, 2CH₂CH₃), 3.22 (q, ⁴J_{H,H} = 6.20 Hz, 4 H, 2CH₂CH₃), 4.34 (d, ²J_{H,H} = 16.2 Hz, 2 H, CH₂), 4.86 (d, ²J_{H,H} = 16.2 Hz, 2 H, CH₂), 6.39 (s, 2 H, H_β, pyridine), 6.93 (m, 4 H, C₆H₄), 7.41 (d, ²J_{H,H} = 6.5 Hz, 2 H, C₆H₄), 7.56 (d, ²J_{H,H} = 6.5 Hz, 2 H, C₆H₄) ppm. ¹³C{¹H} NMR (CD₂Cl₂, 67.83 MHz): δ = 9.6 (CH₂CH₃), 41.9 (CH₂CH₃), 53.8 (CH₂), 101.2, 119.7, 126.2, 127.9, 129.5, 131.0, 149.4, 153.9, 155.2 [C(aryl)], 214.4 (CO) ppm. IR (KBr): $\tilde{\nu}$ = 1948 (vs, CO), 2966 (m, C–H) cm⁻¹. MS (FD⁺, CH₂Cl₂): *m/z* = 512 [Fe(Et₂NpyS₄)₂]⁺, 1024 [Fe(Et₂NpyS₄)₂]⁺. C₂₄H_{25.4}FeN₂O_{1.7}S₄ (552.02): calcd. C 52.17, H 4.62, N 5.07, S 23.21; found C 52.21, H 4.76, N 5.01, S 23.00.

[Fe(CO)(Et₂NpyS₄–H)BF₄] (8a): At –78 °C, (0.013 mL, 0.1 mmol) HBF₄ (54% in Et₂O) was added to a red suspension of **8**·0.7H₂O (50 mg, 0.1 mmol) in CH₂Cl₂ (15 mL). After 1 h of stirring, during the course of which the resultant grey solution was reduced in volume to about 3 mL at –78 °C, addition of *n*-hexane (15 mL) precipitated a grey solid which was isolated and dried in vacuo. Yield: 40 mg (69%) of **8a**. IR (KBr): $\tilde{\nu}$ = 2503 (w, S–H), 1974 (vs, CO) cm⁻¹. MS (FD⁺, CH₂Cl₂): *m/z* = 512 [Fe(Et₂NpyS₄)₂]⁺, 1024 [Fe(Et₂NpyS₄)₂]⁺. C_{24.5}H₂₆FeBClF₄N₂OS₄ (670.49): C 43.86, H 3.91, N 4.17; found C 43.66, H 3.79, N 3.91.

[Fe(CO)(Et₂NpyS₄–Et)BF₄] (8b): A red solution of **8**·0.7H₂O (90 mg, 0.17 mmol) in CH₂Cl₂ (10 mL) was combined with a 1 M Et₃OBF₄ solution in CH₂Cl₂ (0.17 mL, 0.17 mmol). The resultant brown solution was reduced in volume to 3 mL. Addition of Et₂O (20 mL) precipitated a brown solid which was separated by filtration, washed with Et₂O (20 mL) and dried in vacuo. Yield 85 mg of **8b**·0.3CH₂Cl₂ (76%). ¹H NMR (CD₂Cl₂, 269.60 MHz): δ = 0.98 (m, 6 H, 2CH₂CH₃), 1.46 (m, 3 H, CH₂CH₃), 3.12 (m, 6 H, 3CH₂CH₃), 4.48 (m, 2 H, CH₂), 4.90 (m, 2 H, CH₂), 6.43 (d, 2 H,

H_β, pyridine), 7.00 (m, 2 H, C₆H₄), 7.32 (d, 1 H, C₆H₄), 7.61–7.51 (m, 3 H, C₆H₄), 7.74 (m, 1 H, C₆H₄), 8.09 (m, 1 H, C₆H₄) ppm. ¹³C{¹H} NMR (CD₂Cl₂, 67.83 MHz): δ = 12.33 (CH₂CH₃), 13.34 (CH₂CH₃), 41.51 (CH₂CH₃), 44.97 (CH₂CH₃), 55.80, 55.90 (CH₂), 105.38, 105.64, 124.03, 129.69, 129.95, 130.57, 132.22, 132.38, 132.78, 133.61, 133.90, 135.75, 137.14, 152.90, 154.14, 155.48, 156.58 [C(aryl)], 213.24 (CO) ppm. IR (KBr): $\tilde{\nu}$ = 1980 (vs, CO), 1055 (vs, B–F) cm⁻¹. MS (FD⁺, CH₂Cl₂): *m/z* = 512 [Fe(Et₂NpyS₄)₂]⁺, 1024 [Fe(Et₂NpyS₄)₂]⁺. C_{26.3}H_{29.6}FeBCl_{0.6}F₄N₂OS₄ (684.74): C 46.19, H 4.37, N 4.09; found C 46.39, H 4.73, N 4.04.

[Fe(CO)(Et₂NpyS₄–Et)(BF₄)₂] (8c): Et₃OBF₄ (0.40 mL, 0.40 mmol) of a 1 M solution in CH₂Cl₂ was added to a red solution of **8**·0.7H₂O (110 mg, 0.20 mmol) in CH₂Cl₂ (15 mL). The colour immediately changed from red to brown. After 24 h, the reaction mixture was reduced in volume to 3 mL. Addition of Et₂O (30 mL) precipitated a brown solid which was separated by filtration, washed with Et₂O (20 mL) and dried in vacuo. Yield 120 mg of **8c**·0.5CH₂Cl₂ (72%). ¹H NMR (CD₃OD, 269.60 MHz): δ = 1.02–0.97 (t, ³J_{H,H} = 7.2 Hz, 6 H, 2CH₂CH₃), 1.53–1.62 (t, ³J_{H,H} = 7.2 Hz, 6 H, 2CH₂CH₃), 3.21–3.34 (m, 4 H, 2CH₂CH₃), 3.35–3.49 (m, 4 H, CH₂CH₃), 4.79–4.82 (d, ²J_{H,H} = 16.69 Hz, 2 H, CH₂), 5.17–5.23 (d, ²J_{H,H} = 16.70 Hz, 2 H, CH₂), 6.77 (s, 2 H, H_β, pyridine), 7.65 (t, ³J_{H,H} = 7.4 Hz, 3 H, C₆H₄), 7.77 (t, ³J_{H,H} = 7.20/7.60 Hz, 3 H, C₆H₄), 7.97 (d, ²J_{H,H} = 7.64 Hz, 2 H, C₆H₄), 8.32 (d, ²J_{H,H} = 7.83 Hz, 2 H, C₆H₄) ppm. ¹³C{¹H} NMR (CD₃OD, 67.83 MHz): δ = 12.01 (CH₂CH₃), 13.09 (CH₂CH₃), 41.41 (CH₂CH₃), 44.59 (CH₂CH₃), 54.74 (CH₂), 107.23, 133.47, 134.15 134.20, 134.83, 135.42, 136.42, 154.96, 158.00 [C(aryl)], 210.00 (CO) ppm. IR (KBr): $\tilde{\nu}$ = 2007 (vs, CO), 1056 (vs, B–F) cm⁻¹. MS (FD⁺, CH₃OH): *m/z* = 512 [Fe(Et₂NpyS₄)₂]⁺, 1024 [Fe(Et₂NpyS₄)₂]⁺. C_{28.5}H₃₅FeB₂ClF₈N₂OS₄ (814.77): C 42.00, H 4.33, N 3.44, S 15.74; found C 41.68, H 4.57, N 3.64, S 15.98.

[Fe(CNCy)(Et₂NpyS₄)] (9): Cyclohexyl isocyanide (0.032 mL, 0.30 mmol) was added to a yellow suspension of **6** (100 mg, 0.20 mmol) in THF (20 mL). A red solution resulted which was stirred for 12 h, filtered and reduced in volume to about 5 mL. Addition of Et₂O (20 mL) precipitated a red-orange solid which was separated by filtration and dried in vacuo. Yield: 60 mg of **9** (57%). ¹H NMR ([D₈]toluene, 269.60 MHz): δ = 0.39 (t, 6 H, 2CH₂CH₃), 0.93 (t, 10 H, C₆H₁₁), 7.85 (m, 1 H, C₆H₁₁), 2.35 (m, 4 H, 2CH₂CH₃), 3.98–3.92 (d, 2 H, CH₂), 4.85–4.80 (d, 2 H, CH₂), 5.68 (s, 2 H, H_β, pyridine), 6.68–6.83 (m, 4 H, C₆H₄), 7.53–7.24 (m, 2 H, C₆H₄), 7.80 (d, 2 H, C₆H₄) ppm. IR (KBr): $\tilde{\nu}$ = 2105 (vs, CN), 2969, 2932 (m, C–H) cm⁻¹. MS (FD⁺, toluene): *m/z* = 512 [Fe(Et₂NpyS₄)₂]⁺, 620 [Fe(CNCy)(Et₂NpyS₄)₂]⁺, 1024 [Fe(Et₂NpyS₄)₂]⁺. C₃₀H₃₅FeN₃S₄ (621.73): calcd. C 57.95, H 5.67, N 6.76, S 20.63; found C 57.34, H 6.21, N 6.77, S 20.43.

[Fe(NO)(Et₂NpyS₄)BF₄] (10). a) From **8:** Solid NOBF₄ (5 mg, 0.04 mmol) was added to a red solution of **8**·0.7H₂O (20 mg, 0.04 mmol) in CH₂Cl₂ (10 mL). During the course of 10 min, a yellow-green solution resulted which was filtered and reduced in volume to about 5 mL. Addition of Et₂O (20 mL) precipitated a yellow-green solid which was separated by filtration and dried in vacuo. Yield: 15 mg of **10**·CH₂Cl₂·Et₂O (65%). **b) From **6**:** At 0 °C, solid NOBF₄ (5 mg, 0.04 mmol) was added to a yellow suspension of **6** (20.5 mg, 0.04 mmol) in CH₂Cl₂ (10 mL). After stirring at 0 °C for 70 min and at room temperature for 30 min, the resultant yellow-green mixture was filtered, reduced in volume to about 5 mL and combined with Et₂O (20 mL). The resultant green solid was separated by filtration and dried in vacuo. Yield: 18 mg **10**·CH₂Cl₂·Et₂O (82%). ¹H NMR (CD₂Cl₂, 269.60 MHz): δ = 1.05

(t, 6 H, 2CH₂CH₃), 3.25 (q, 4 H, 2CH₂CH₃), 4.46 (d, 2 H, CH₂), 5.00 (m, 2 H, CH₂), 6.46 (s, 2 H, H_β², pyridine), 7.28 (m, 4 H, C₆H₄), 7.45 (m, 2 H, C₆H₄), 7.65 (d, 2 H, C₆H₄) ppm. ¹³C{¹H} NMR (CD₂Cl₂, 67.83 MHz): δ = 11.9 (CH₂CH₃), 45.1 (CH₂CH₃), 55.1 (CH₂), 106.2, 126.26, 128.1, 129.5, 131.1, 132.1, 151.3, 152.7, 156.65 [C(aryl)] ppm. IR (KBr): ν̄ = 1882 (vs, NO), 1081 (vs, B-F) cm⁻¹. MS (FD⁺, CH₂Cl₂): m/z = 512 [Fe(Et₂NpyS₄)]⁺, 1024 [{Fe(Et₂NpyS₄)₂]⁺. C₂₈H₃₆BrCl₂F₄FeN₃OS₄ (788.42): calcd. C 42.65, H 4.60, N 5.33, found C 42.68, H 4.21, N 5.76.

[Fe(NO)(Et₂NpyS₄)] (11): By means of a syringe, NO gas (5 mL, 0.21 mmol) was injected into a stirred yellow suspension of **6** (80 mg, 0.158 mmol) in CH₂Cl₂ (20 mL). A brown mixture resulted which was stirred for 24 h, filtered and reduced in volume to about 5 mL. Addition of Et₂O (20 mL) precipitated a brown solid which was separated by filtration and dried in vacuo. Yield: 78 mg **11**·0.5CH₂Cl₂ (92%). IR (KBr): ν̄ = 1637 (s, NO) cm⁻¹. MS (FD⁺, CH₂Cl₂): m/z = 512 [Fe(Et₂NpyS₄)]⁺, 544 [Fe(NO)(Et₂NpyS₄)]⁺, 1024 [{Fe(Et₂NpyS₄)₂]⁺. C_{23.5}H₂₅ClFeN₃OS₄ (565.15): calcd. C 48.25, H 4.31, N 7.18; found C 48.77, H 4.49, N 7.11.

[Fe(N₂H₄)(Et₂NpyS₄)] (12): N₂H₄ (0.032 mL, 1.0 mmol) was added to a yellow suspension of **6** (100 mg, 0.20 mmol) in CH₂Cl₂ (15 mL). During the course of 48 h, a deep red solution resulted which was filtered and reduced in volume to about 2 mL. Addition of Et₂O (20 mL) precipitated a brown solid which was separated by filtration and dried in vacuo. Yield: 60 mg of **12**·0.25Et₂O (55%). ¹H NMR ([D₈]THF, 269.60 MHz): δ = 0.85 (t, 6 H, 2CH₂CH₃), 2.90 (br., N₂H₄), 3.32 (m, 4 H, 2CH₂CH₃), 4.50 (m, 4 H, 2CH₂), 6.56 (s, 2 H, H_β, pyridine), 7.44 (m, 2 H, C₆H₄), 7.94 (m, 2 H, C₆H₄), 9.72 (m, 4 H, C₆H₄) ppm. IR (KBr): ν̄ = 3318, 3285, 3237 (m, N-H) cm⁻¹. MS (FD⁺, THF): m/z = 512 [Fe(Et₂NpyS₄)]⁺, 1024 [{Fe(Et₂NpyS₄)₂]⁺. C₂₄H_{30.5}FeN₄OS₄ (563.13): calcd. C 51.19, H 5.46, N 9.95; found C 50.82, H 5.71, N 9.55.

[Ru(NO)(Et₂NpyS₄)]Br (13): Over the course of 1 h, a solution of Bu₄N[Ru(NO)(S₂C₆H₄)₂] (2.5 g, 3.82 mmol) in THF (30 mL) was added dropwise to a boiling solution of **3**·0.16 THF (1.52 g, 4.52 mmol) in THF (30 mL). The mixture was heated to reflux for a further 1 h and cooled to room temperature. After 2 h, the precipitated red solid was separated by filtration, washed with THF (30 mL), ether (20 mL) and dried in vacuo. Yield 2 g of **13**·0.3THF (77%). ¹H NMR ([D₆]DMSO, 269.60 MHz): δ = 0.92 (t, 6 H, 2CH₂CH₃), 3.20 (q, 4 H, 2CH₂CH₃), 4.94 (d, 2 H, CH₂), 5.25 (d, 2 H, CH₂), 6.67 (s, 2 H, H_β, pyridine), 7.28 (m, 4 H, C₆H₄), 7.52 (d, 2 H, C₆H₄), 7.99 (d, 2 H, C₆H₄) ppm. ¹³C{¹H} NMR (CD₂Cl₂, 67.83 MHz): δ = 13.85 (CH₂CH₃), 44.00 (CH₂CH₃), 54.83 (CH₂), 104.62, 124.96, 128.51, 129.73, 130.72, 132.87, 149.86, 151.80, 156.19 [C(aryl)] ppm. IR (KBr): ν̄ = 1858 (vs, NO) cm⁻¹. MS (FD⁺, CH₂Cl₂): m/z = 558 [Ru(Et₂NpyS₄)]⁺, 585 [Ru(NO)(Et₂NpyS₄)]⁺, 1116 [[Ru(Et₂NpyS₄)₂]⁺. C_{24.3}H_{28.6}BrN₃O₂RuS₄ (704.3): calcd. C 41.49, H 4.10, N 5.97; found C 41.37, H 4.48, N 6.18.

[{Ru(Et₂NpyS₄)₂] (14): NH₃ gas was bubbled through a red solution of **13**·0.3THF (110 mg, 0.16 mmol) in MeOH (10 mL) for 1 h. The green solid which precipitated was separated by filtration, washed with MeOH (10 mL), Et₂O (10 mL) and dried in vacuo. Yield 140 mg, **14**·H₂O (42%). IR (KBr): ν̄ = 2967, 2923 (m, C-H) cm⁻¹. MS (FD⁺, DMSO): m/z = 1116 [{Ru(Et₂NpyS₄)₂]⁺. C₄₆H₅₀N₄ORuS₈ (1115.53): C 48.74, H 4.44, N 4.94; found C 48.70, H 4.14, N 4.85.

[Ru(N₂H₄)(Et₂NpyS₄)] (15): N₂H₄ (0.5 mL, 16 mmol) was added to a red-brown suspension of **13**·0.3THF (110 mg, 0.16 mmol) in THF (10 mL). Gas evolved and a red solution formed which was concentrated in volume to 3 mL. Addition of MeOH (10 mL) led to precipitation of a red microcrystalline solid which was separated, washed with MeOH (10 mL) and ether (20 mL) then dried in vacuo. Yield 40 mg of **15**·0.3 N₂H₄·0.6H₂O (41%). ¹H NMR ([D₆]DMSO, 269.60 MHz): δ = 1.02–0.83 (t, 6 H, 2CH₂CH₃), 3.10–2.99 (m, 4 H, 2CH₂CH₃), 3.30 (m, 1 H, NH₂), 4.24–4.22 (d, 1 H, NH₂), 4.31–4.28 (d, 2 H, CH₂), 4.37 (d, 2 H, CH₂), 4.42 (d, 1 H, NH), 6.19 (s, 2 H, H_β, pyridine), 6.67–6.59 (m, 4 H, C₆H₄), 7.37–7.35 (m, 2 H, C₆H₄), 7.50–7.47 (m, 2 H, C₆H₄) ppm. ¹³C{¹H} NMR (DMF-d₇, 67.83 MHz): δ = 12.02 (CH₂CH₃), 43.25 (CH₂CH₃), 56.69 (CH₂), 102.93, 119.93, 130.61, 132.19, 132.98, 149.98, 158.28 [C(aryl)] ppm. IR (KBr): ν̄ = 3318, 3242, 3100 (m, N-H) cm⁻¹. MS (FD⁺, CH₂Cl₂): m/z = 558 [Ru(Et₂NpyS₄)]⁺, 590 [Ru(N₂H₄)(Et₂NpyS₄)]⁺, 1116 [{Fe(Et₂NpyS₄)₂]⁺. C_{23.5}H_{29.7}N_{3.3}O_{0.6}RuS₄ (611.5): calcd. C 45.17, H 4.89, N 10.69, S 20.97; found C 45.16, H 5.07, N 10.53, S 20.63.

X-ray Structure Determination of [Fe(Et₂NpyS₄-O₂)]₂·8CDCl₃ (7·8CDCl₃), [Fe(CO)(Et₂NpyS₄)·CDCl₃ (8·CDCl₃), [Fe(CNCy)(Et₂NpyS₄)·2THF (9·2THF), [Fe(NO)(Et₂NpyS₄)]BF₄·CH₂Cl₂ (10·CH₂Cl₂), [Fe(N₂H₄)(Et₂NpyS₄)] (12), [Ru(N₂H₄)(Et₂NpyS₄)] (15) and [Ru(N₂H₄)(Et₂NpyS₄)]·N₂H₄ (15·N₂H₄): Red-brown blocks of 7·8CDCl₃ were grown at room temperature from a saturated CDCl₃ solution of **7** over one week. Red blocks of 8·CDCl₃ were grown at room temperature from a saturated CDCl₃ solution of **8** over 3 d. Red single-crystals of 9·2THF were grown at -27 °C from a saturated THF solution of **9** over 5 weeks. Brown blocks of 10·CH₂Cl₂ were obtained from a saturated CH₂Cl₂ solution at room temperature over 4 weeks. Brown single-crystals of **12** were grown at room temperature from a saturated CD₂Cl₂ solution over 2 weeks. Red prisms of **15** were grown at room temperature from a saturated THF solution over one week. Orange single crystals of 15·N₂H₄ were grown at room temperature from a saturated THF solution of **15** over one week in the presence of excess hydrazine. Suitable single-crystals were embedded in protective perfluoropolyether oil. Data were collected either with a Siemens P4 (7·8CDCl₃) or a Nonius-KappaCCD diffractometer (8·CDCl₃, 9·2THF, 10·CH₂Cl₂, **12**, **15** and 15·N₂H₄) using Mo-K_α radiation (λ = 71.073 pm, graphite monochromator). Intensity data were corrected for absorption effects using either ψ-scans^[18] (7·8CDCl₃) or multiple scans of equivalent reflections (SADABS^[19] for 9·2THF and SORTAV^[20] for 8·CDCl₃, **12**, **15** and 15·N₂H₄) while for 10·CH₂Cl₂ absorption effects were neglected. The structures were solved by direct methods and refined on F² using full-matrix least-squares procedures (SHELXTL NT 5.10^[21] for 7·8CDCl₃, 8·CDCl₃, 9·2THF, **12**, **15** and 15·N₂H₄ or SHELXTL NT 6.12^[22] for 10·CH₂Cl₂). Hydrogen atoms were either located in a difference Fourier map and refined with a common fixed isotropic displacement parameter (7·8CDCl₃, 8·CDCl₃, **12**), kept fixed in their positions with a common fixed isotropic displacement parameter (**15**, 15·N₂H₄), or were geometrically positioned (9·2THF, 10·CH₂Cl₂). The solvate molecules in the structures of 7·8CDCl₃, 8·CDCl₃, 9·2THF and 10·CH₂Cl₂ are partly disordered. Table 6 lists selected crystallographic data. CCDC-238453 (7·8CDCl₃), -238454 (8·CDCl₃), -238455 (9·2THF), -238456 (10·CH₂Cl₂), -238457 (**12**), -238458 (**15**) and -238459 (15·N₂H₄) contain the supplementary crystallographic data for this paper. These data can be obtained free of charge at www.ccdc.cam.ac.uk/conts/retrieving.html [or from the Cambridge Crystallographic Data Centre, 12 Union Road, Cambridge CB2 1EZ, UK; Fax: (internat.) + 44-1223-336-033; E-mail: deposit@ccdc.cam.ac.uk]

Table 6. Crystallographic data and structure refinement details for $[\{\text{Fe}(\text{Et}_2\text{NpyS}_4-(\text{O}_2)_2\}_2] \cdot 8\text{CHCl}_3$ (**7**·8CHCl₃), $[\text{Fe}(\text{CO})(\text{Et}_2\text{NpyS}_4)] \cdot \text{CDCl}_3$ (**8**·CDCl₃), $[\text{Fe}(\text{CNCy})(\text{Et}_2\text{NpyS}_4)] \cdot 2\text{THF}$ (**9**·2THF), $[\text{Fe}(\text{NO})(\text{Et}_2\text{NpyS}_4)]\text{BF}_4 \cdot \text{CH}_2\text{Cl}_2$ (**10**·CH₂Cl₂), $[\text{Fe}(\text{N}_2\text{H}_4)(\text{Et}_2\text{NpyS}_4)]$ (**12**) $[\text{Ru}(\text{N}_2\text{H}_4)(\text{Et}_2\text{NpyS}_4)]$ (**15**) and $[\text{Ru}(\text{N}_2\text{H}_4)(\text{Et}_2\text{NpyS}_4)] \cdot \text{N}_2\text{H}_4$ (**15**·N₂H₄)

	7 ·8CDCl ₃	8 ·CDCl ₃	9 ·2THF	10 ·CH ₂ Cl ₂	12	15	15 ·N ₂ H ₄
Empirical formula	C ₅₄ H ₄₈ Cl ₂₄ D ₈ Fe ₂ N ₄ O ₄ S ₈	C ₂₅ H ₂₄ Cl ₃ D ₈ Fe ₂ N ₂ O ₄ S ₄	C ₃₈ H ₅₁ FeN ₃ O ₂ S ₄	C ₂₄ H ₂₆ BCl ₂ F ₄ FeN ₃ OS ₄	C ₂₃ H ₂₈ FeN ₄ S ₄	C ₂₃ H ₂₈ N ₄ RuS ₄	C ₂₃ H ₃₂ N ₆ RuS ₄
<i>M_r</i> [g mol ⁻¹]	2052.06	569.91	756.91	714.28	544.58	589.80	621.86
Crystal size [mm]	0.50 × 0.28 × 0.15	0.20 × 0.15 × 0.05	0.49 × 0.28 × 0.10	0.20 × 0.07 × 0.05	0.25 × 0.21 × 0.14	0.38 × 0.22 × 0.12	0.17 × 0.17 × 0.04
<i>F</i> (000)	1028	1352	1624	728	2272	2416	1280
Crystal system	triclinic	monoclinic	monoclinic	triclinic	orthorhombic	orthorhombic	monoclinic
Space group	<i>P</i> $\bar{1}$	<i>P</i> ₂ / <i>n</i>	<i>P</i> ₂ / <i>n</i>	<i>P</i> $\bar{1}$	<i>Pbca</i>	<i>Pbca</i>	<i>P</i> ₂ / <i>n</i>
<i>a</i> [pm]	1168.6(1)	1286.76(3)	1595.4(2)	933.94(5)	1194.52(2)	1199.83(3)	1091.05(8)
<i>b</i> [pm]	1305.7(1)	1316.25(3)	1320.8(2)	1208.46(7)	1899.01(3)	1922.54(4)	1312.29(8)
<i>c</i> [pm]	1521.6(1)	1642.96(4)	1799.0(3)	1417.81(7)	2111.16(4)	2105.70(4)	1806.19(8)
<i>α</i> [°]	99.91(1)	90	90	82.880(4)	90	90	90
<i>β</i> [°]	111.80(1)	96.347(2)	101.088(7)	75.627(4)	90	90	96.562(5)
<i>γ</i> [°]	98.77(1)	90	90	67.638(4)	90	90	90
<i>V</i> [nm ³]	2.0632(3)	2.7656(2)	3.7201(9)	1.4328(2)	4.7890(2)	4.8573(2)	2.5691(3)
<i>Z</i>	1	4	4	2	8	8	4
<i>ρ</i> _{calcd.} [g cm ⁻³]	1.652	1.585	1.368	1.656	1.511	1.613	1.608
<i>μ</i> [mm ⁻¹]	1.375	1.161	0.668	1.057	0.999	1.009	0.961
<i>T</i> [K]	210	100	100	100	100	100	100
θ range [°]	1.9–26.01	3.34–29.00	3.46–25.68	3.15–25.00	6.01–30.00	3.3–30	3.47–27.50
Measured reflections	9209	46227	35439	18296	33984	47848	24316
Unique reflections	7971	7346	6961	5037	6926	7017	5867
<i>R</i> _{int}	0.0392	0.1189	0.1036	0.1415	0.0808	0.1335	0.1031
Observed reflections	5274	4691	4587	3507	5040	716	4038
σ criterion	<i>I</i> > 2σ(<i>I</i>)	<i>I</i> > 2σ(<i>I</i>)	<i>I</i> > 2σ(<i>I</i>)	<i>I</i> > 2σ(<i>I</i>)	<i>I</i> > 2σ(<i>I</i>)	<i>I</i> > 2σ(<i>I</i>)	<i>I</i> > 2σ(<i>I</i>)
Refined parameters	551	419	509	389	373	289	307
<i>R_i</i> [<i>I</i> > 2σ(<i>I</i>)]	0.0518	0.0468	0.0592	0.0651	0.0384	0.0445	0.0451
<i>wR</i> ₂ (all data)	0.1084	0.1092	0.1472	0.1871	0.0871	0.0892	0.0897
Absorption correction	0.505/0.613	0.850/0.957	0.795/1.000	–	0.723/0.937	0.807/0.885	0.888/0.972
<i>T</i> _{min.} / <i>T</i> _{max.}							

Acknowledgments

We thank Prof. Dr. Horst Kisch and Prof. Dr. Andreas Grohman for their helpful suggestions. Financial support for this work from the Deutsche Forschungsgemeinschaft (SFB, 583: “Redoxaktive Metallkomplexe”) and the Fonds der Chemischen Industrie is gratefully acknowledged.

[1] [1a] B. K. Burgess, in “Molybdenum Enzymes, Cofactors and Model Systems” (Eds.: E. I. Stiefel, D. Coucouvanis, W. E. Newton), *ACS Symp. Ser.* **1993**, 535, 144–170. [1b] D. J. Lowe, R. N. F. Thorneley, B. E. Smith, in *Metalloproteins*, part 1 (“Metal Proteins with Redox Roles”) (Ed.: P. Harrison), Verlag Chemie, Weinheim, **1985**. [1c] R. R. Eady, in *Perspectives in Bioinorganic Chemistry* (Eds.: R. W. Hay, J. R. Dilworth, K. B. Nolan), JAI Press, London, **1991**, p. 225.

[2] [2a] D. Sellmann, N. Blum, F. W. Heinemann, *Z. Naturforsch., Teil B* **2001**, 56, 581–588. [2b] D. Sellmann, N. Blum, F. W. Heinemann, B. A. Hess, *Chem. Eur. J.* **2001**, 7, 1874–1880. [2c] D. Sellmann, J. Utz, N. Blum, F. W. Heinemann, *Coord. Chem. Rev.* **1999**, 190–192, 607–627. [2d] D. Sellmann, D. Häußinger, T. Gottschalk-Gaudig, F. W. Heinemann, *Z. Naturforsch., Teil B* **2000**, 55, 723–729. [2e] D. Sellmann, K. Engl, F. W. Heine-

mann, *Eur. J. Inorg. Chem.* **2000**, 423–429. [2f] D. Sellmann, J. Utz, F. W. Heinemann, *Inorg. Chem.* **1999**, 38, 5314–5322.

[2g] D. Sellmann, K. Hein, F. W. Heinemann, *Eur. J. Inorg. Chem.* **2004**, 3136–3146.

[3] [3a] R. A. Henderson, G. J. Leigh, C. J. Pickett, *Adv. Inorg. Chem. Radiochem.* **1983**, 27, 197–292. [3b] H. Kandler, C. Gauss, W. Bidell, S. Rosenberger, T. Bürgi, I. L. Eremenko, D. Veghini, O. Orama, P. Burger, H. Berke, *Chem. Eur. J.* **1995**, 1, 541–548. [3c] J. Chatt, A. J. Pearman, R. L. Richards, *J. Organomet. Chem.* **1975**, 101, 45–47.

[4] D. Sellmann, B. Hautsch, A. Rösler, F. W. Heinemann, *Angew. Chem.* **2001**, 113, 1553–1555; *Angew. Chem. Int. Ed.* **2001**, 40, 1505–1507.

[5] D. Sellmann, A. Hille, F. W. Heinemann, M. Moll, A. Rösler, J. Sutter, G. Brehm, M. Reiher, B. A. Hess, S. Schneider, *Inorg. Chim. Acta* **2003**, 348, 194–198.

[6] N. Blum, PhD Dissertation, University of Erlangen-Nürnberg, **2000**.

[7] H. Takato, J. Kankare, *Acta Chem. Scand., Ser. B* **1987**, 41, 219–221.

[8] [8a] M. J. Baker-Hawkes, D. Billig, H. B. Gray, *J. Am. Chem. Soc.* **1966**, 88, 4870–4875. [8b] D. Sellmann, S. Fünfgelder, G. Pohlmann, F. Knoch, M. Moll, *Inorg. Chem.* **1990**, 29, 4772–4778. [8c] D. Sellmann, S. Fünfgelder, F. Knoch, M. Moll, *Z. Naturforsch., Teil B* **1991**, 46, 1601–1608. [8d] D.

- Sellmann, P. Bail, F. Knoch, M. Moll, *Chem. Ber.* **1995**, *128*, 653–663. ^[8c] D. Sellmann, P. Bail, F. Knoch, M. Moll, *Inorg. Chim. Acta* **1995**, *237*, 137–141.
- ^[9] ^[9a] A. T. Laurie, C. N. Juan, M. O. Marilyn, K. M. Pradip, *Inorg. Chem.* **1998**, *38*, 616–617. ^[9b] C. A. Ghilardi, S. Midolini, S. Moneti, *J. Organomet. Chem.* **1981**, *217*, 391–401. ^[9c] K. Manoj, C. J. Gerard, R. O. Day, J. M. Michael, *J. Am. Chem. Soc.* **1989**, *111*, 8323–8325.
- ^[10] ^[10a] F. Bottomley, *Acc. Chem. Res.* **1978**, *11*, 158–163. ^[10b] J. A. McCleverty, *Chem. Rev.* **1979**, *79*, 53–76.
- ^[11] D. Sellmann, G. Binker, *Z. Naturforsch., Teil B* **1987**, *42*, 341–347.
- ^[12] ^[12a] D. Sellmann, K. P. Peters, F. W. Heinemann, *Eur. J. Inorg. Chem.* **2004**, 581–590. ^[12b] D. Sellmann, J. Sutter, *Inorg. Chem.* **2004**, *52*, 587–681.
- ^[13] P. L. Bogdan, M. Sabat, S. A. Sunshine, C. Woodcock, D. F. Shriver, *Inorg. Chem.* **1988**, *27*, 1904–1910.
- ^[14] L. Pauling, *Die Natur der chemischen Bindung*, VCH Verlagsgesellschaft, Weinheim, **1973**, p. 249.
- ^[15] R. R. Gagne, C. A. Koval, G. C. Linsensky, *Inorg. Chem.* **1980**, *19*, 2855–2857.
- ^[16] A. J. Bond, L. R. Faulkner, *Electrochemical Methods, Fundamentals and Applications*, Wiley, New York, **1980**.
- ^[17] J. Degani, R. Fochi, *Synthesis* **1976**, *7*, 471–472.
- ^[18] A. C. T. North, D. C. Phillips, F. S. Mathews, *Acta Crystallogr., Sect. A* **1968**, *24*, 351–359.
- ^[19] R. H. Blessing, *Acta Crystallogr., Sect. A* **1995**, *51*, 33–38.
- ^[20] SADABS: Bruker AXS, Inc., Madison, WI, USA, **2002**.
- ^[21] SHELXTL NT 5.10: Bruker AXS, Inc., Madison, WI, USA, **1998**.
- ^[22] SHELXTL NT 6.12: Bruker AXS, Inc., Madison, WI, USA, **2002**.

Received May 14, 2004

Early View Article

Published Online October 20, 2004